Tribol Lett (2016) 64:32
DOI 10.1007/s11249-016-0764-x

ORIGINAL PAPER

Wear Characteristics of Mo-W-Type Hot-Work Steel at High Temperature

Shuang Li[1,2,3] · Xiaochun Wu[1,2,3] · Xinxin Li[1] · Junwan Li[1,2,3] · Xijuan He[1,2,3]

Received: 14 May 2016 / Accepted: 27 September 2016 / Published online: 13 October 2016

Abstract The friction and wear characteristics of new Mo-W-type hot-work die steel, known as SDCM-S, were studied at high temperature. The results showed that the new Mo-W-type steel had greater wear resistance compared with H13 steel, which was due to its high oxidizability and high-temperature property. The high oxidizability and high temper stability features facilitate the generation, growth, and maintenance of a tribo-oxide layer at high temperature under relatively stable conditions. The thick tribo-oxide layer and high temper stability postpone the transition from mild to severe wear and ensure that conditions of mild oxidative wear are maintained in SDCM-S steel. The M_2C and M_6C carbides in Mo-W-type steel increase the temper stability and provide sufficient additional support for the formation and growth of a single thick tribo-oxide layer at high temperature. Mild oxidative wear is the dominant wear mechanism for SDCM-S steel between 400 and 700 °C.

Keywords Wear characteristic · Oxidative wear · Hot-work die steel · Carbides

✉ Junwan Li
lijunwan@shu.edu.cn

[1] State Key Laboratory of Advanced Special Steel, Shanghai University, Shanghai 200072, China

[2] Shanghai Key Laboratory of Advanced Ferrometallurgy, Shanghai University, Shanghai 200072, China

[3] School of Materials Science and Engineering, Shanghai University, Shanghai 200072, China

1 Introduction

Hot-work die steels are widely used in manufacturing industries for applications such as hot-forging, press-hardening and die-casting, where the dies endure high temperatures and mechanical loads [1–4]. The high-temperature oxidative wear is the main failure mechanism of the die in these applications. This is the predominant wear mechanism for the majority of engineering metallic components subjected to high ambient temperature [5–10]. Oxidative wear occurs frequently when metals or steels are subjected to high temperature. Quinn et al. [11, 12] first proposed the model of oxidative wear, while Hsu et al. [13] proposed classifications of mild and severe wear. The oxidative wear was identified by the existence of tribo-oxides on the worn surface in some previous studies [14–17] and could present different wear characteristics despite the existence of tribo-oxides [18]. Hsu et al. [19] categorized the oxidative wear of metal into mild and severe oxidative wear. Under mild oxidative wear conditions, the wear rate is relatively low. However, under severe oxidative wear conditions, the wear rate is high, which may lead to premature wear failure of the hot-work die. Under harsh conditions, the transition from mild to severe wear often occurs because of dry sliding friction, particularly at high temperature [20–23]. This transition not only occurs on the sliding of steel but also takes place on the friction and tribo-oxidation wear of metal alloys [24–26]. The severe oxidative wear should be limited or avoided during the service life of hot-work die steel. Therefore, controlling and avoiding the transition from mild to severe oxidative wear has great theoretical significance for engineering applications involving materials. The high-temperature wear characteristic is closely related to the tribo-oxide and matrix [27, 28]. Mild oxidative wear

behavior is closely related to the degree of tribo-oxidation, as well as the thickness of the tribo-oxide layer. Some studies demonstrated that the wear behavior depend on tribo-oxidation, rather than the microstructure of the steel matrix [29–31]. However, mild oxidative wear will not be maintained when significant softening occurs in the substrate beneath the oxide at high temperature [32]. Materials with high oxidizability can easily form oxides and tribo-oxide layers during sliding. Meanwhile, large plastic deformation is avoided and the tribo-oxide layer is preserved in the materials with high temper stability. Therefore, mild oxidative wear can be maintained for steels with high temper stability and oxidizability.

The purpose of this letter is to clarify the friction and wear behaviors of Mo-W-type hot-working die steel at high temperature. Molybdenum and tungsten are the main alloy elements in high-speed steel materials, and they make sure the steels have higher wear resistance and excellent red hardness [33, 34]. The high-temperature wear resistances of the new Mo-W- type hot-working die steel and H13 steel were studied as a function of temperature.

2 Experimental

AISI H13 steel is a conventional Cr–Mo-V-type hot-work die steel, which is used to produce hot-press casting and forging dies. A new Mo-W- type hot-work die steel, known as SDCM-S, has been developed with high wear performance at high temperature. Table 1 shows the compositions of the SDCM-S steel and commercial AISI H13 steel.

The initial heat treatment process is described in the following paragraphs. First, the SDCM-S steel samples were austenitized at 1080 °C for 45 min, quenched in oil, and then tempered twice at 600 °C for 2 h to achieve tempered martensite. This resulted in a hardness value of 52.2 ± 0.4 HRC (about 537 HV). The H13 steel samples were austenitized at 1030 °C for 30 min, quenched in oil, and then tempered twice at 520 °C for 2 h to achieve tempered martensite. This resulted in a hardness value of 52.8 ± 0.6 HRC (544 HV). Their microstructures are shown in Fig. 1.

The plate sample had dimensions of 10 × 10 × 35.5 mm. Following the heat treatment, the samples were ground to remove the oxide layer, and subsequently cleaned with ethanol and air dried. Ball-on-plate reciprocating dry sliding wear tests were conducted using a UMT-3 high-temperature wear tester; a schematic of the wear tester is shown in Fig. 2. The ball material consisted of SiC ceramic. The ball had a diameter of 9.525 mm and its hardness was 2800 HV at room temperature. The test parameters were as follows: 400, 500, 600, 700 °C for the surrounding temperature; 10 N for the normal load; 5 HZ for the sliding frequency; 0.1 m/s for the sliding velocity; and 360 m for the sliding distance. The wear rate, W_R, is calculated by the equation $W_R = V/NL$, where V is the wear volume (mm^3), N is the load (N), and L is the sliding distance (m). The wear volumes were measured using an optical profilometer (ContourGT-K1; Bruker, USA). The average values obtained from two or three samples are presented.

Table 1 Chemical composition of SDCM-S and H13 steel (wt%)

	C	Mn	Si	Cr	W	Mo	V
SDCM-S	0.35–0.40	0.10	0.04	0.12	1.5–2.0	4.5–5.0	0.02
H13	0.38	1.5	1.1	5.3	–	1.4	0.9

The oxidizability of steel has an important role in determining its oxidative wear. In this work, static oxidation tests were performed on SDCM-S and H13 steels within an S2-5-12-type resistance furnace at temperatures of 500 and 700 °C for 1, 3, 7, and 10 h, under dry air conditions. Oxidation resistance is evaluated by the weight gain rate after oxidation testing. The weight gain rate, W, is calculated using the formula $W = (W_i - W_0)/S$, where W_0 and W_i are the weights of the samples (mg) before and after the oxidation test, respectively. S denotes the superficial area (mm^2).

The microstructures of the steels were examined using a scanning electron microscope (SEM; ZEISS Supra40 type, Germany) and transmission electron microscope (TEM; JEOL2010F, Japan) equipped with an energy dispersive spectral (EDS) analyzer under an operating voltage of 200 kV. For the TEM examination, thin foil samples were cut, ground, and subsequently dimpled via final ion thinning using a double-jet electro-polisher at low temperature. The morphology, composition, and microstructure of the worn surface and subsurface were examined by SEM. Phases on the worn surfaces were identified by a 18KW-D/MAX2500V+/PC type X-ray diffractometer (XRD) with CuKα radiation and a secondary beam graphite monochromator. The hardness distributions of the cross-sectioned worn surface were measured by a Vickers microhardness tester with a load of 100 g force. The Vickers hardness values were measured at least five positions using a digital micro-hardness tester (MH-3, China), and the average values are presented.

3 Results and Discussion

The friction coefficients of two types of hot-work steels during the sliding period at various temperatures are presented in Fig. 3, which shows that the SDCM-S steel has a lower friction coefficient compared with that of the H13 steel. At 400 and 700 °C, the average friction coefficient

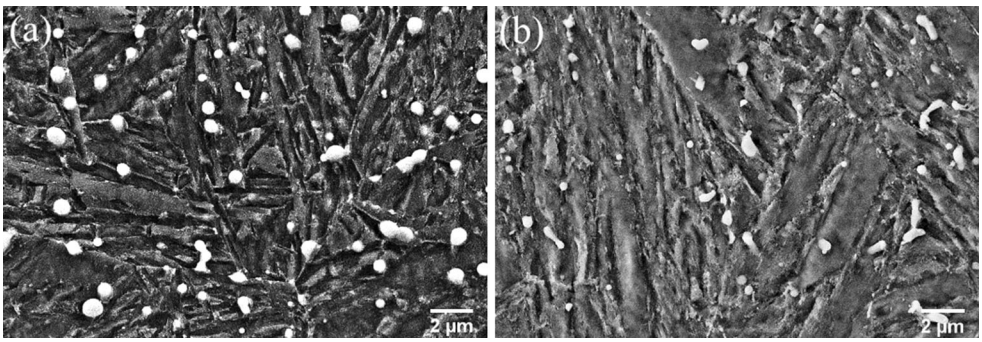

Fig. 1 Microstructures of die steels: **a** SDCM-S, **b** H13

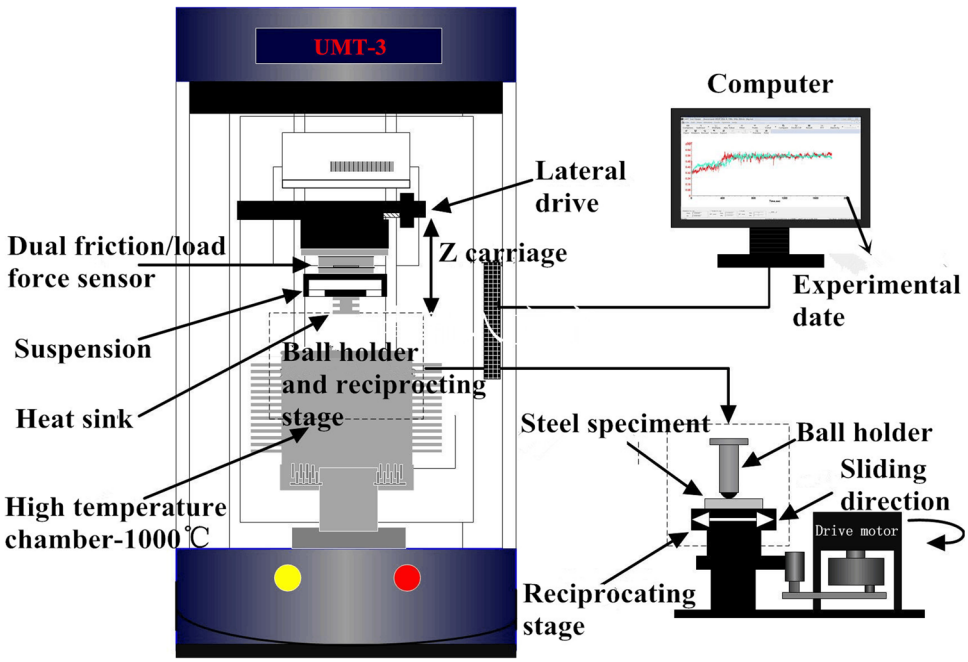

Fig. 2 Schematic diagram of the wear tester

values of the SDCM-S are obviously lower than those of the H13 steels. The friction coefficient of the SDCM-S steel is slightly lower than that of the H13 steel at 500 and 600 °C.

The wear rates of the SDCM-S and H13 steels at different temperatures are shown in Fig. 4. The wear rate of the SDCM-S steel is lower than that of the H13 steel at all test temperatures. The Mo-W type SDCM-S steel has superior wear resistance compared with the H13 steel. The wear rate of the SDCM-S steel changes slightly as the temperature is varied. However, the H13 steel exhibits a greater wear rate under the same test parameters. The wear rate of the H13 steel is slightly greater than that of the SDCM-S steel at 400 and 500 °C. When the ambient temperature rises to 600 and 700 °C, the H13 steel exhibits a high wear rate; however, the wear rate of the SDCM-S steel is still low. The wear rate initially decreases and subsequently increases as the temperature is increased for both steels. These observations suggest that the two steels exhibit different wear mechanisms during sliding.

Some researcher claimed that the high-temperature wear behaviors and mechanisms of the steels are closely related to the tribo-oxide and matrix [12, 15]. Tribo-oxidation results in a reduction of the wear rate when the matrix keeps sufficient strength to support the tribo-oxide layer. Under this condition, the degree of reduced wear depends on the amount of tribo-oxide or the thickness of the tribo-oxide layer.

Oxides have a remarkable influence on the friction and wear behavior of steels and alloys [8, 35, 36]. The weight gain rate associated with oxidation can be used as an indicator to assess the oxidizability of steel [37]. Curves, as presented in Fig. 5a, b, show the oxidation weight gain as a function of time at 500 and 700 °C. The quantity of oxide increases as the temperature and holding time are

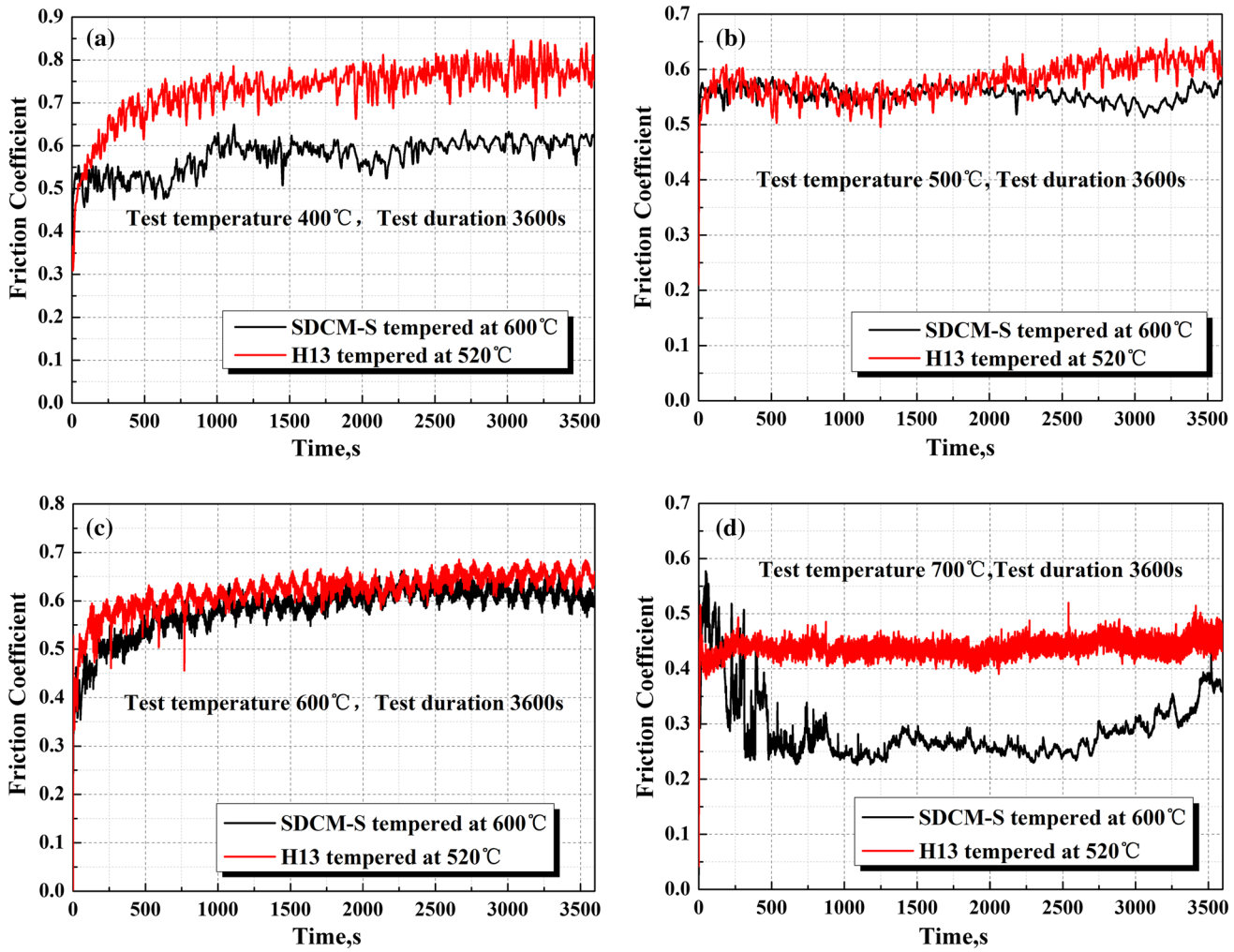

Fig. 3 Friction coefficient of tested steels at **a** 400 °C, **b** 500 °C, **c** 600 °C and **d** 700 °C

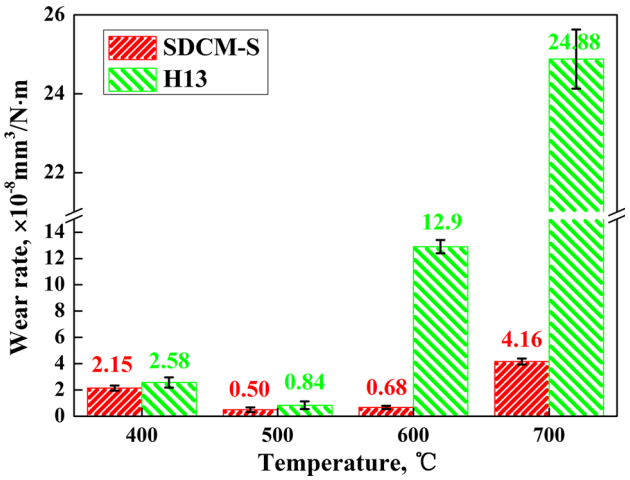

Fig. 4 Wear rates of two steels at different temperatures

increased. The SDCM-S steel exhibits more serious oxidation than that of H13 steel. We know that the oxidation resistance of steel increases as the Cr content increases, which directly affects the weight gain rate of oxidation under certain conditions. Therefore, the SDCM-S steel, with no Cr content, exhibits greater oxidizability compared with the H13 steel which has a greater Cr content (5.5 %). It can form more oxides during the sliding process at high temperature.

X-ray diffraction patterns for worn surfaces of the steels sliding under various conditions are shown in Fig. 6. The results for SDCM-S steel are shown in Fig. 6a. Trace tribo-oxides (Fe_3O_4 and Fe_2O_3) were identified on worn surfaces. As the ambient temperature increases, the amount of tribo-oxides increases. The amount of tribo-oxides in SDCM-S steel was more than that in H13 steel at all test temperature. The peak corresponding to oxide phases of oxides in SDCM-S steel significantly surpassed the peaks of the iron phase when the temperature was above 500 °C. Tribo-oxidation reduces the friction coefficient of the steel by forming a protective layer [21]. The SDCM-S steel has higher oxidizability and this results in more tribo-oxidation

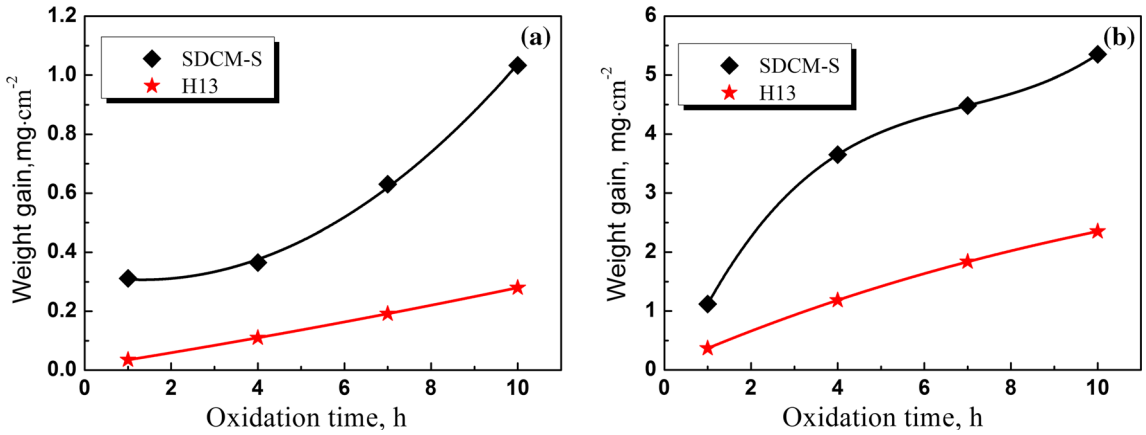

Fig. 5 The weight gain *curves* for various holding time of two steels at **a** 500 °C and **b** 700 °C

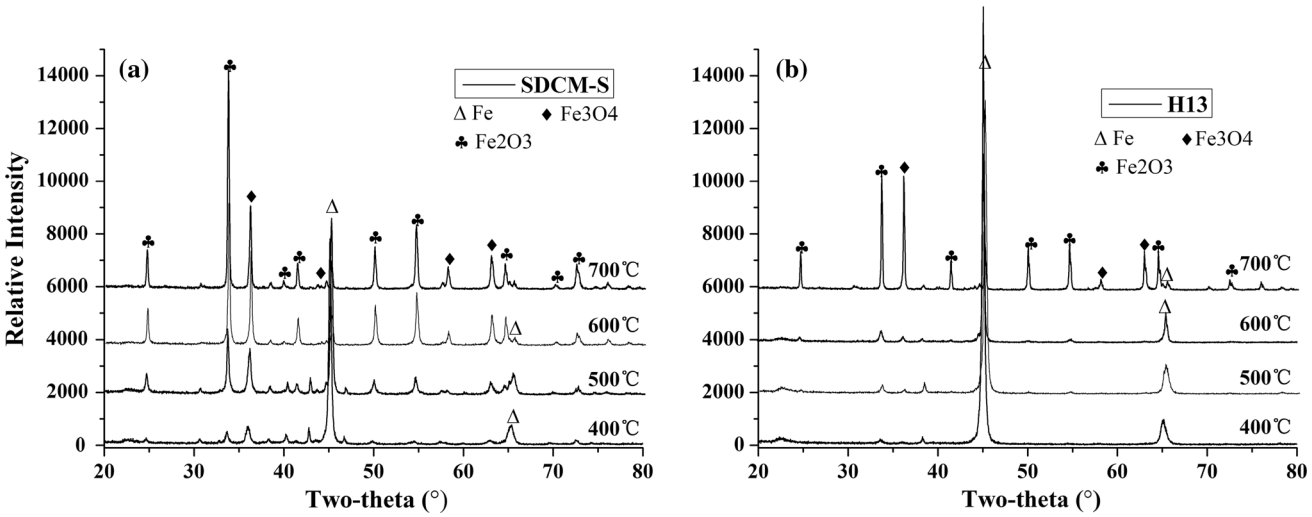

Fig. 6 X-ray diffraction patterns for worn surfaces of test steels sliding under various conditions

during sliding compared with the H13 steel. Therefore, the friction coefficients of SDCM-S steel are lower than those of H13 steel.

The wear mechanisms can be clarified by thoroughly examining the morphology, composition, and structure of the worn surface and subsurface at different temperatures. The worn surfaces and subsurfaces were presented in various states and with different characteristics, which were related to the wear mechanism of the material [27].

The SEM images of the worn surface and subsurface morphologies are shown in Figs. 7 and 8. At 400 °C, the tribo-oxide covered the worn surface of the SDCM-S steel. In certain areas, a patch-like tribo-oxide layer with a smooth surface exists on the worn surface, as shown in Fig. 7a, b. The patches like tribo-oxide are metallic particles which are oxidized and then agglomerated and compacted in the friction contact as well as particles of oxides which are also agglomerated and compacted in the friction contact. Under the same conditions, the tribo-oxide on the worn surface of the H13 steel is less than that of the SDCM-S steel, as shown in Fig. 8a, b. For both steels, the existence of tribo-oxides could be observed within the morphological images of the worn surface and subsurface at 400 °C. This shows that in this study oxidative wear prevailed for both steels; however, differences could be observed in the mount and cover rate of tribo-oxidation and the size of the area covered by the tribo-oxide patch. The SDCM-S steel, with high oxidizability, could form a greater amount of oxide compared with the H13 steel, as illustrated above. Therefore, for the SDCM-S steel, the degree of tribo-oxidation, as well as the area covered by the tribo-oxide patch, was greater.

The mount and cover rate of tribo-oxidation increased as the surrounding temperature increased. At 500 °C, Fig. 7a, b shows that the worn surface of the SDCM-S steel is entirely covered with a single tribo-oxide layer. The morphology of the worn surface consists of smooth

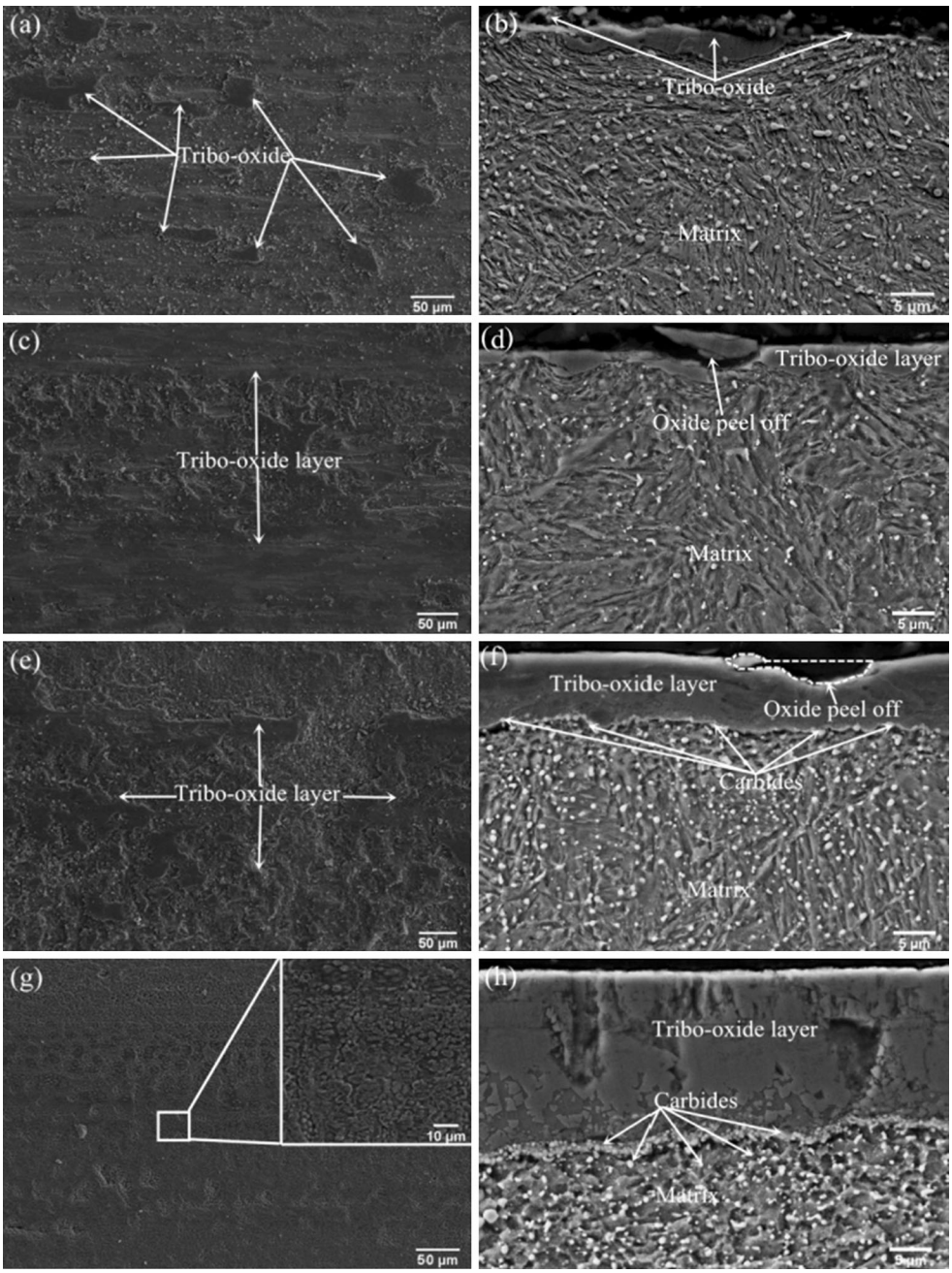

Fig. 7 The worn surface and subsurface of SDCM-SS steel at **a**, **b** 400 °C, **c**, **d** 500 °C, **e**, **f** 600 °C, and **g**, **h** 700 °C

undelaminated and delaminated regions. The tribo-oxide layers tend to crack due to a fatigue mechanism and are likely to spall off during the sliding process; with the result that wear debris and delaminated craters are generated on the worn surface. Stott et al. [30] described the role of tribo-oxide layers as 'glazes', which form on the sliding surfaces during frictional contact. The glazed layers can temporarily protect surfaces from further contact damage. If the glazes wear off, new glazes are formed to replace them. This alternated of formation, loss, and reformation can lead to short-term friction or wear transients. This phenomenon is similar to that associated with the friction coefficient fluctuation, as shown in Fig. 3. Meanwhile, the degree of tribo-oxidation on the worn surface of the H13 steel increases and a large tribo-oxide patch (maximum thickness of 7 μm) is formed at 500 °C, as presented in Fig. 8c, d. Due to a fatigue mechanism, the tribo-oxide layer will crack and subsequently spall off, as shown in Fig. 7d. This represents the physical process of wear loss and is defined as typical mild oxidative wear [11, 12, 38]. The wear rate decreased because of the presence of a single tribo-oxide layer. The mild oxidative wear prevailed when

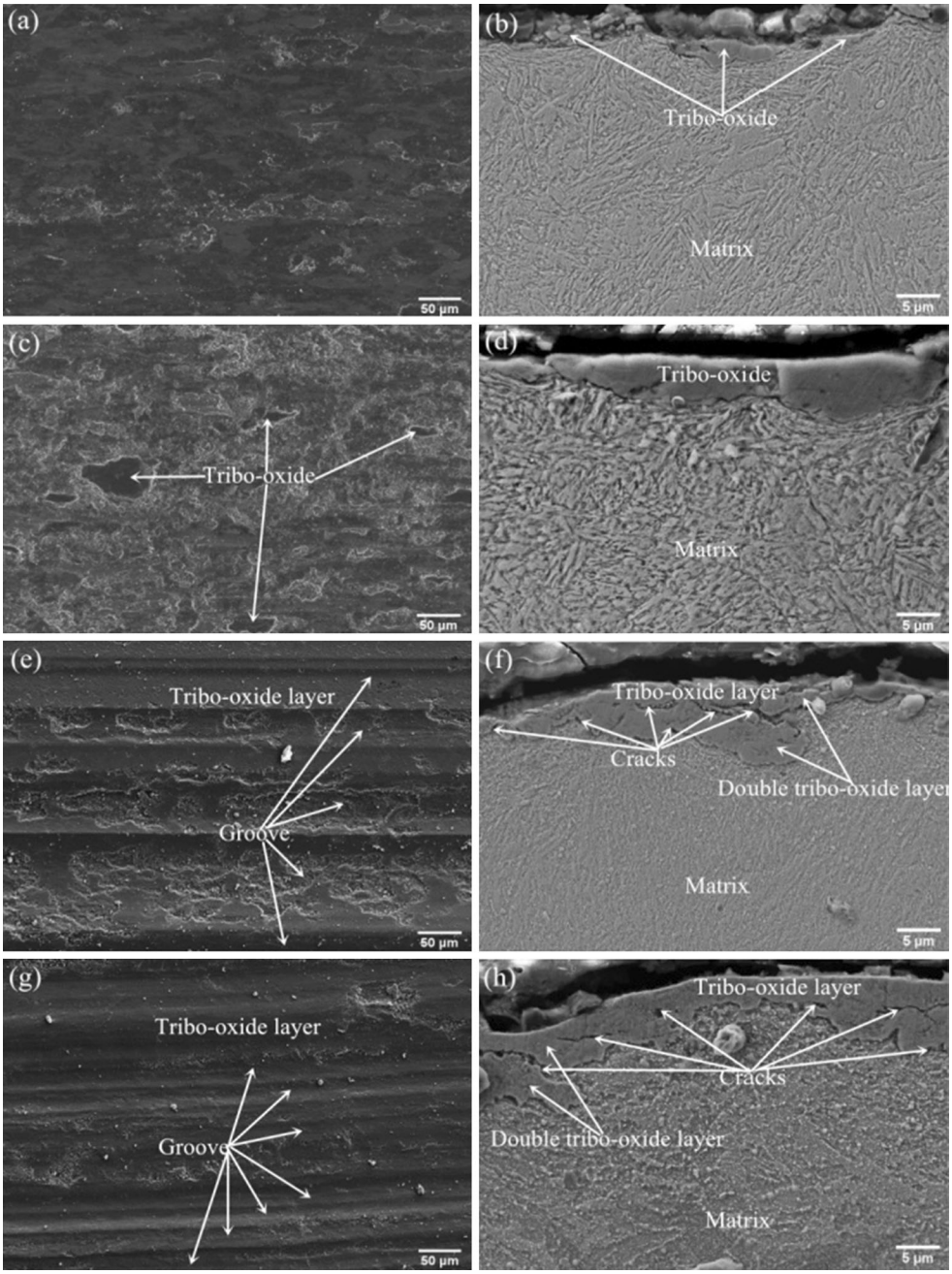

Fig. 8 The worn surface and subsurface of H13 steel at **a**, **b** 400 °C, **c**, **d** 500 °C, **e**, **f** 600 °C, and **g**, **h** 700 °C

the single oxide layer reached a certain thickness and the degree of subsurface plastic deformation was low [39]. The degree of tribo-oxidation of the H13 steel was lower than that of the SDCM-S steel. However, the cover rate of the tribo-oxide patch increased compared with that at 400 °C. This explains why the wear rate of the H13 steel was at its lowest at 500 °C. The single tribo-oxide layer did not completely cover the worn surface. Therefore, the friction coefficient of the H13 steel was still higher than that of the SDCM-S steel.

The single tribo-oxide layer was preserved on the worn surface of the SDCM-S steel when the temperature was 600 °C, as shown in Fig. 7e, f. In this case, mild oxidative wear prevailed and a thicker tribo-oxide layer formed on the worn surface. However, the morphology of the worn surface of the H13 steel is obviously different to that of the SDCM-S steel. Figure 8e shows the presence of valley-like groove traces on the worn surface. Figure 8f shows the appearance of many cracks in the tribo-oxide layer. Meanwhile, the tribo-oxide layer grows deeply into the

matrix in some regions. Many cracks propagate into the inner surface and subsurface of the tribo-oxide layer. The thickness of the tribo-oxide layer was inhomogeneous and a double tribo-oxide layer formed during the sliding process. This type of oxidative wear was referred to as a transition from mild to severe oxidative wear by previous researchers [20, 23, 24]. Although the tribo-oxide layer entirely covers the worn surfaces of both steels, the H13 steel has a higher wear rate.

At 700 °C, the worn surface of the SDCM-S steel is similar to that observed at 600 °C. The tribo-oxide layer of the SDCM-S steel exhibited characteristics of a single layer, and no cracks formed between the tribo-oxide layer and the matrix, as shown in Fig. 7g, h. Figure 8g, h presents the morphology of the worn surface of the H13 steel at 700 °C. The tribo-oxide layer grows deeply into the matrix and forms a double tribo-oxide layer in some regions. Cracks are generated at the internal tribo-oxide layer and between the tribo-oxide layer and the matrix.

It has been reported that a harder matrix can support the tribo-oxide layer more effectively than a soft matrix [40]. Friction results in plastic deformation and frictional heat during sliding. The strain and temperature gradients cause dynamic changes in the microstructure and properties of the substructure, which affect the wear behavior [41]. Figure 9 shows that the microstructure distribution is away from the worn surface of SDCM-S steel. The recovery degree of the subsurface microstructure decreased as the depth increased. The frictional heating and high surrounding temperature generate a higher temperature on the worn surface, and, consequently, the tribo-oxide layer beneath the substrate softens. The hardness distribution curves can reflect the softening of the subsurface matrix. The decrease of hardness in the first micrometers of the surface is due to the common influence of mechanical softening (friction forces) and thermal softening. During sliding, the high ambient temperature and friction heat lead to the high temperature on the worn surface. This results in the recovery and recrystallization of the deformed substrate at subsurface. In the cases of 400 and 500 °C, a large part of the surface softening could also be attributed to mechanical softening. The AISI H11 steel (which is close

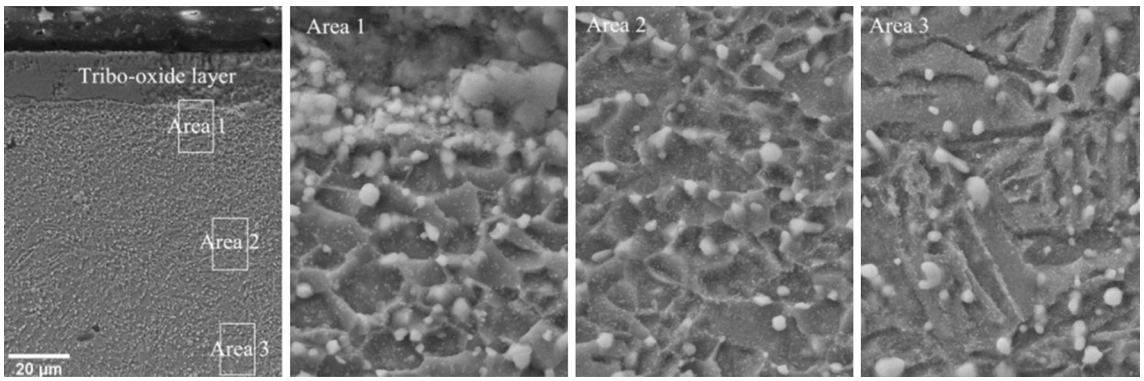

Fig. 9 Subsurface microstructure distributions of SDCM-S steels after the test

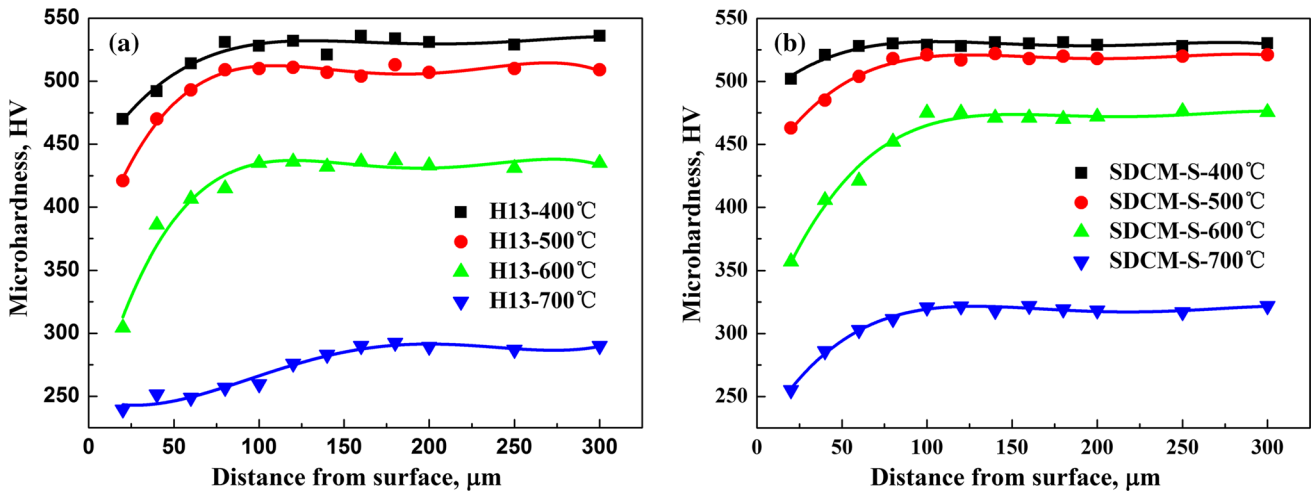

Fig. 10 Hardness distribution away from the worn surface of **a** H13 and **b** SDCM-S steels

in composition to AISI H13) is prone to thermal and also to mechanical softening [42].

Figure 10 illustrates the microhardness distributions of the two steels after the test. The hardness decreases from the matrix towards the worn surface. Following sliding, the degree of reduction in hardness differs for the two materials. Following testing at temperatures of 400 and 500 °C, the hardness of the steel decreases to a certain extent; however, the matrices of both steels maintained a relatively high level of hardness. Under these conditions, the reduction in wear correlates with the degree of tribo-oxidation and thickness of the tribo-oxide layer. The reduction in wear due to tribo-oxidation still depends on the degree of tribo-oxidation and the thickness of the tribo-oxide layer. The SDCM-S steel with greater oxidizability forms more tribo-oxide on the worn surface compared with H13 steel. Therefore, the SDCM-S steel had a lower friction coefficient and wear rate than the H13 steel at 400 and 500 °C.

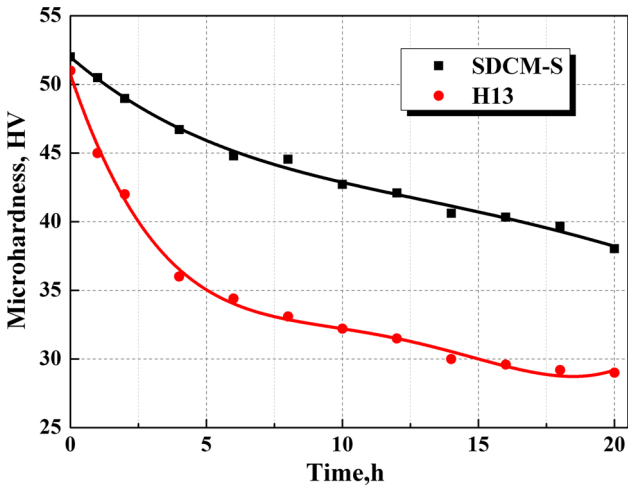

Fig. 11 The hardness *curves* for various tempering times of tested steels at 620 °C

The tribo-oxide completely covered the worn surface of the H13 steel; however, its hardness significantly decreased at 600 °C, as shown in Fig. 10b. The SDCM-S steel has better temper stability performance at high temperature compared with the H13 steel. Figure 11 shows the hardness curves of the steels that were tempered at 620 °C for various times. The SDCM-SS steel shows better temper stability compared with the H13 steel. Following holding at 650 °C for 24 h, the hardness of the SDCM-SS steel was approximately 9 HRC greater than that of the H13 steel. Therefore, the SDCM-S steel can sufficiently support the formation and maintenance of a single tribo-oxide layer. It is likely that the high temper stability ensures that the matrix has sufficient strength to support the formation of a defect-free tribo-oxide layer that can cover the entire worn surface. Under these conditions, the H13 steel presented severe oxidative wear; however, the SDCM-S steel still exhibited mild oxidative wear. This explains why there was an obvious increase in the wear rate of the H13 steel when the temperature was 600 °C.

At 700 °C, there was a severe decrease in the hardness of both steel grades. A high degree of thermal softening and plastic deformation directly accelerates the delamination of the tribo-oxide. For both steels, the surrounding temperature and frictional heating accelerated the recovery of the subsurface microstructure, which resulted in an obvious decrease of the matrix hardness. This is why the wear rate of the two steels increased at 700 °C. However, the hardness of the SDCM-S steel was still greater than that of the H13 steel. This is because many fine M_2C secondary carbides precipitated during tempering, which can postpone the recovery process and the softening of the martensite microstructure, as shown in Fig. 12a, b. Therefore, the SDCM-S steel can maintain a higher hardness compared with the H13 steel. The softened matrix tends to lead to large plastic deformation and cracks are generated and propagate during sliding. As the cracks grow to a critical size, delamination of the matrix occurs, which

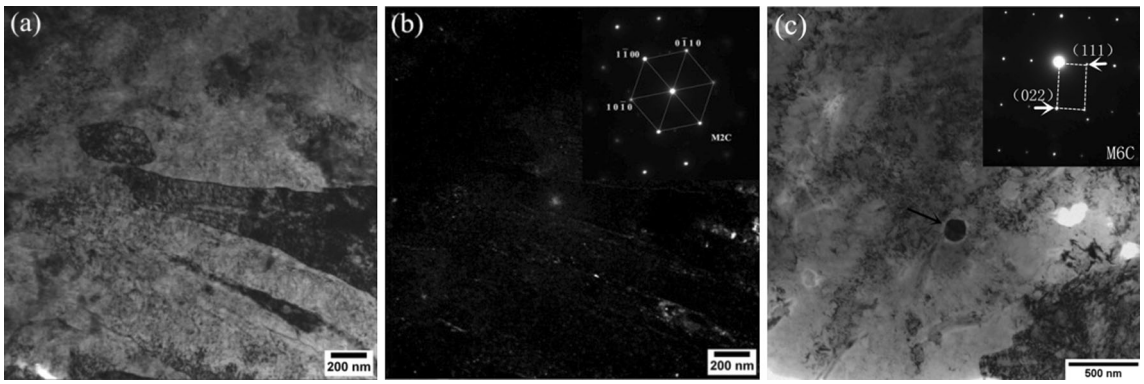

Fig. 12 TEM micrographs of bright image of (**a**) dark filled images (**b**) of M2C carbide and bright filled images (**c**) of M6C carbides in SDCM-S steel

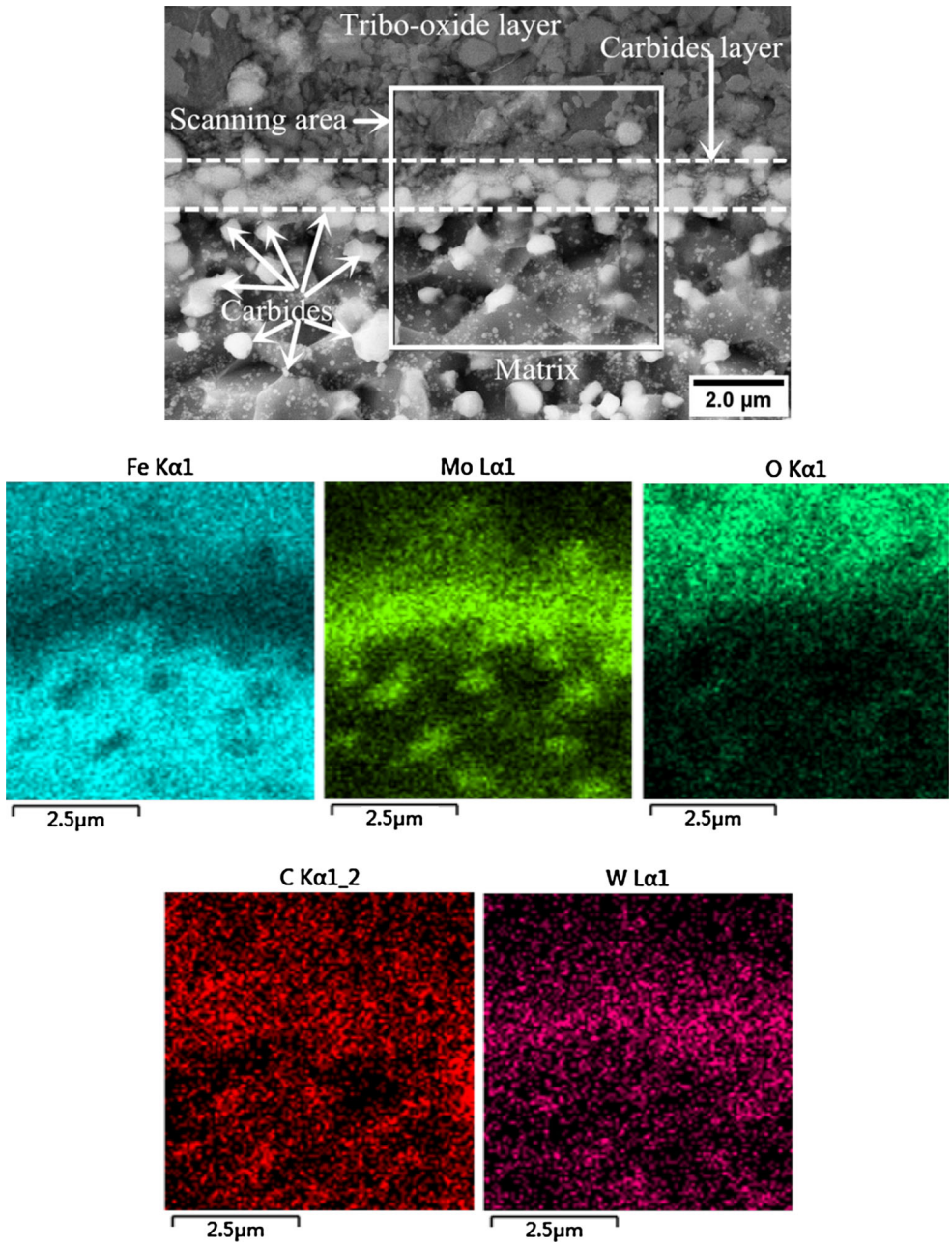

Fig. 13 The microstructure of subsurface and the energy dispersive X-ray spectrometry line-by-line scanning analysis

results in a greater wear rate [43]. The oxide grows deeply into the matrix, forming a double tribo-oxide layer in some regions under these conditions. Subsequently, cracks propagate to the inner tribo-oxide layer and between the tribo-oxide layer and the matrix. The oxides grew deeply into the matrix, and a double tribo-oxide layer formed in some regions. Severe oxidative wear prevailed for the H13 steel under this condition. In contrast, the cross-sections and morphologies of the worn surface and subsurface of the SDCM-S steel revealed the existence of a single tribo-oxide layer on the worn surface. Therefore, a mild wear mechanism and low wear rate were still maintained for the SDCM-S steel in this temperature region.

It is important to study the subsurface microstructure of the SDCM-S steel at 700 °C. There were many fine and large-sized carbides in the subsurface matrix of the SDCM-S steel. The hard second phase particles are the most important parameter for determining the wear resistance of the steel at low temperature, and can protect the matrix against wear [44]. With regard to oxidative wear, the function of the carbides depends on their influence on the matrix. Secondary phases can affect the sliding wear by

hardening the matrix. It can be observed that the microstructures differ for the SDCM-S and H13 steels, as shown in Figs. 7h and 8h. The cross-section of the worn surface of the H13 steel consisted of a tribo-oxide layer and an affected matrix. However, an additional assembled carbide layer could be observed in the cross-section of the worn surface of the SDCM-S steel, as shown in Fig. 13, which shows the results of the energy dispersive X-ray spectrometry line-by-line scanning analysis performed on the cross-section of the worn subsurface. It also shows that the molybdenum and tungsten content of the assembled carbide layer was significantly higher than that of the matrix.

This layer may have formed via the aggregation of carbides during sliding. These carbides, M_2C and M_6C shown in Fig. 12a–c, respectively, with high size stability and hardness, would support the tribo-oxide layer and impede the growth of oxides into the matrix. The large-sized M_6C acts as the foundation pile on the matrix, which prevents the small-sized carbide being taken away by the oxide during sliding and provides support to the tribo-oxide layer. Meanwhile, these carbides have a strong cohesive bond with the metallic matrix and cannot be easily removed because this would cause delamination of the tribo-oxide layer. At the same time, the high thermodynamic stability of these carbides can hinder further oxygen diffusion into matrix. Therefore, the assembled carbides can impede the growth of the tribo-oxide layer into the matrix. These features illustrate that the influence of carbide on the oxidative wear is not just on the matrix but it also has a significant effect on the tribo-oxide layer. Although the hardness of the SDCM-S steel matrix at 700 °C is low, the assembled carbide layer can provide sufficient additional support for the formation and growth of a single thick tribo-oxide layer. Thus, at 700 °C, the SDCM-S steel exhibits mild oxidative wear and a low wear rate with a single thick layer.

At 400 and 500 °C, both types of steel exhibited mild oxidative wear. The substrate had sufficient hardness to provide support to the tribo-oxide patch or layer. The SDCM-S steel has higher oxidizability and forms more tribo-oxides during the sliding process compared with H13 steel. Therefore, the SDCM-S steel has a lower wear rate and friction coefficient.

Owing to its high temper stability, the SDCM-S steel maintained its high hardness at 600 °C, and, therefore, the single tribo-oxide layer could be effectively supported. However, the hardness of the H13 steel significantly decreased. This facilitated the generation and propagation of cracks within and beneath the tribo-oxide layer. Consequently, the mild oxidative wear was not maintained and severe oxidative wear occurred, which resulted in a high wear rate. A similar, but more severe, phenomenon occurred for the H13 steel when the temperature increased to 700 °C.

At 700 °C, the SDCM-S steel can still support the single tribo-oxide layer on the worn surface. The high temper stability postpones the transition from mild to severe wear. The assembled carbide layer plays an important role under these conditions. The carbide layers improve the support provided to the tribo-oxide layer, obstruct the entry of oxygen into the matrix, and impede the growth of the tribo-oxide layer. Such factors ensure that the predominant wear mechanism of the SDCM-S steel remains mild oxidative wear and the wear resistance of the SDCM-S steel is higher than that of the H13 steel at high temperature.

4 Conclusion

1. The SDCM-S steel has greater wear resistance compared with the H13 steel.
2. The high oxidizability of the SDCM-S steel facilitates the generation and growth of the tribo-oxide layer at high temperature. The high temper stability postpones the transition from mild to severe wear, and conditions of mild oxidative wear are maintained for long periods at high temperature. The combination of these factors results in the high wear resistance of the SDCM-S steel.
3. The carbides in SDCM-S steel can provide sufficient additional support for the formation and growth of a single thick tribo-oxide layer.
4. Mild oxidative wear is the predominant wear mechanism for the SDCM-S steel between 400 and 700 °C.

Acknowledgments This work supported by the National Natural Science Foundation of China (Grant Nos. 51401117 and 51171104). The authors would like to thank Na. Min from Instrumental Analysis and Research Center of Shanghai University for the help with the TEM measurements.

References

1. Barrau, O., Boher, C., Gras, R., Rezai-Aria, F.: Analysis of the friction and wear behaviour of hot work tool steel for forging. Wear **255**, 1444–1454 (2003)
2. Boher, C., Le, R.S., Penazzi, L., Dessain, C.: Experimental investigation of the tribological behavior and wear mechanisms of tool steel grades in hot stamping of a high-strength boron steel. Wear **294–295**, 286–295 (2012)
3. Fontalvo, G.A., Mitterer, C.: The effect of oxide-forming alloying elements on the high temperature wear of a hot work steel. Wear **258**, 1491–1499 (2005)
4. Terek, P., Kovačević, L., Miletić, A., Panjan, P., Baloš, S., Škorić, B., et al.: Effects of die core treatments and surface finishes on the sticking and galling tendency of Al–Si alloy casting during ejection. Wear **356–357**, 122–134 (2016)

5. Blau, P.J.: Elevated-temperature tribology of metallic materials. Tribol. Int. **43**, 1203–1208 (2010)
6. Pellizzari, M., Cescato, D., De Flora, M.G.: Hot friction and wear behaviour of high speed steel and high chromium iron for rolls. Wear **267**, 467–475 (2009)
7. Hernandez, S., Hardell, J., Winkelmann, H., Ripoll, M.R., Prakash, B.: Influence of temperature on abrasive wear of boron steel and hot forming tool steels. Wear **338–339**, 27–35 (2015)
8. Cui, X.H., Wang, S.Q., Wang, F., Chen, K.M.: Research on oxidation wear mechanism of the cast steels. Wear **265**, 468–476 (2008)
9. Marui, E., Hasegawa, N., Endo, H., Tanaka, K., Hattori, T.: Research on the wear characteristics of hypereutectoid steel. Wear **205**, 186–199 (1997)
10. Stott, F.H., Glascott, J., Wood, G.C.: Factors affecting the progressive development of wear-protective oxides on iron-base alloys during sliding at elevated temperatures. Wear **97**, 93–106 (1984)
11. Quinn, T.F.J.: Review of oxidational wear. Tribol. Int. **16**, 257–271 (1983)
12. Quinn, T.F.J.: Review of oxidational wear part II: recent developments and future trends in oxidational wear research. Tribol. Int. **16**, 305–315 (1983)
13. Hsu, S.M., Shen, M.C., Ruff, A.W.: Wear prediction for metals. Tribol. Int. **30**, 377–383 (1997)
14. Wei, M.X., Chen, K.M., Wang, S.Q., Cui, X.H.: Analysis for wear behaviors of oxidative wear. Tribol. Lett. **42**, 1–7 (2011)
15. Quinn, T.F.J., Winer, W.O.: The thermal aspects of oxidational wear. Wear **102**, 67–80 (1985)
16. Straffelini, G., Pellizzari, M., Maines, L.: Effect of sliding speed and contact pressure on the oxidative wear of austempered ductile iron. Wear **270**, 714–719 (2011)
17. Tewari, A.: Load dependence of oxidative wear in metal/ceramic tribocouples in fretting environment. Wear **289**, 95–103 (2012)
18. Rainforth, W.M., Leonard, A.J., Perrin, C., Bedolla-Jacuinde, A., Wang, Y., Jones, H., et al.: High resolution observations of friction-induced oxide and its interaction with the worn surface. Tribol. Int. **35**, 731–748 (2002)
19. Hsu, S.M., Shen, M.C., Ruff, A.W.: Wear prediction for metals. Tribol. Int. **30**, 377–383 (1997)
20. Wang, S.Q., Wang, L., Zhao, Y.T., Sun, Y., Yang, Z.R.: Mild-to-severe wear transition and transition region of oxidative wear in steels. Wear **306**, 311–320 (2013)
21. Kato, H.: Severe–mild wear transition by supply of oxide particles on sliding surface. Wear **255**, 426–429 (2003)
22. Viáfara, C.C., Sinatora, A.: Influence of hardness of the harder body on wear regime transition in a sliding pair of steels. Wear **267**, 425–432 (2009)
23. Wang, S.Q., Wei, M.X., Wang, F., Cui, X.H., Dong, C.: Transition of mild wear to severe wear in oxidative wear of H21 steel. Tribol. Lett. **32**, 67–72 (2008)
24. Wang, L., Zhang, Q.Y., Li, X.X., Cui, X.H., Wang, S.Q.: Severe-to-mild wear transition of titanium alloys as a function of temperature. Tribol. Lett. **53**, 511–520 (2014)
25. Lebedeva, I.L., Presnyakova, G.N.: Adhesion wear mechanisms under dry friction of titanium alloys in vacuum. Wear **148**, 203–210 (1991)
26. Straffelini, G., Molinari, A.: Mild sliding wear of Fe–0.2 % C, Ti–6 % Al–4 % V and Al-7072: a comparative study. Tribol. Lett. **41**, 227–238 (2011)
27. Wang, S.Q., Wei, M.X., Zhao, Y.T.: Effects of the tribo-oxide and matrix on dry sliding wear characteristics and mechanisms of a cast steel. Wear **269**, 424–434 (2010)
28. Lim, S.C.: The relevance of wear-mechanism maps to mild-oxidational wear. Tribol. Int. **35**, 717–723 (2002)
29. Batchelor, A.W., Stachowiak, G.W., Cameron, A.: The relationship between oxide films and the wear of steels. Wear **113**, 203–223 (1986)
30. Stott, F.H.: The role of oxidation in the wear of alloys. Tribol. Int. **31**, 61–71 (1998)
31. Straffelini, G., Trabucco, D., Molinari, A.: Oxidative wear of heat-treated steels. Wear **250**, 485–491 (2001)
32. Zhang, Q.Y., Chen, K.M., Wang, L., Cui, X.H., Wang, S.Q.: Characteristics of oxidative wear and oxidative mildwear. Tribol. Int. **61**, 214–223 (2013)
33. Garza-Montes-de-Oca, N.F., Rainforth, W.M.: Wear mechanisms experienced by a work roll grade high speed steel under different environmental conditions. Wear **267**, 441–448 (2009)
34. Yan, X.G., Li, D.Y.: Effects of the sub-zero treatment condition on microstructure, mechanical behavior and wear resistance of W9Mo3Cr4V high speed steel. Wear **302**, 854–862 (2013)
35. Chen, Y., Tang, Y., Zhang, H., Fu, L.: Effect of chromium on oxidation in wear of surface nanocrystalline martensite steel. Tribol. Lett. **61**, 1–7 (2016)
36. Stott, F.H., Wood, G.C.: The influence of oxides on the friction and wear of alloys. Tribol. Int. **11**, 211–218 (1978)
37. Wei, M.X., Wang, S.Q., Chen, K.M., Cui, X.H.: Relations between oxidative wear and Cr content of steels. Wear **272**, 110–121 (2011)
38. Sullivan, J.L., Quinn, T.F.J., Rowson, D.M.: Developments in the oxidational theory of mild wear. Tribol. Int. **13**, 153–158 (1980)
39. Wei, M.X., Wang, S.Q., Wang, L., Cui, X.H., Chen, K.M.: Effect of tempering conditions on wear resistance in various wear mechanisms of H13 steel. Tribol. Int. **44**, 898–905 (2011)
40. Saka, N., Pamies-Teixeira, J.J., Suh, N.P.: Wear of two-phase metals. Wear **44**, 77–86 (1977)
41. Wang, Y., Lei, T., Liu, J.: Tribo-metallographic behavior of high carbon steels in dry sliding: III. Dynamic microstructural changes and wear. Wear **231**, 20–37 (1999)
42. Boher, C., Barrau, O., Gras, R., Rézai- Aria, F.: A wear model based on cumulative cyclic plastic straining. Wear **267**, 1087–1094 (2009)
43. Abouei, V., Saghafian, H., Kheirandish, S.: Effect of microstructure on the oxidative wear behavior of plain carbon steel. Wear **262**, 1225–1231 (2007)
44. Vardavoulias, M.: The role of hard second phases in the mild oxidational wear mechanism of high-speed steel-based materials. Wear **173**, 105–114 (1994)